Journal of Molecular Catalysis A: Chemical 416 (2016) 10–19

Contents lists available at ScienceDirect

Journal of Molecular Catalysis A: Chemical

journal homepage: www.elsevier.com/locate/molcata

Encapsulation of SALEN- and SALHD-Mn(III) complexes in an Al-pillared clay for bicarbonate-assisted catalytic epoxidation of cyclohexene

Ana M. Garcia [a], Viviana Moreno [b], Sonia X. Delgado [a], Alfonso E. Ramírez [b], Luis A. Vargas [b], Miguel Á. Vicente [c], Antonio Gil [d], Luis A. Galeano [a,*]

[a] Research Group on Functional Materials and Catalysis (GIMFC), Department of Chemistry, Nariño University, Calle 18 Cra. 50, Campus Torobajo, Pasto, Nariño, Colombia
[b] Research Group Catalysis, Department of Chemistry, Cauca University, Sector Tulcán-Edificio Antiguo Liceo, Carrera 3 No. 3N-100, Popayán, Cauca, Colombia
[c] Department of Inorganic Chemistry, Salamanca University, Plaza la Merced s/n, E-37008 Salamanca, Spain
[d] Department of Applied Chemistry, Los Acebos Building, Public University of Navarre, Campus Arrosadía, E-31006 Pamplona, Spain

ARTICLE INFO

Article history:
Received 17 September 2015
Received in revised form 30 January 2016
Accepted 30 January 2016
Available online 11 February 2016

Keywords:
Catalytic epoxidation
Encapsulated catalysts
Immobilized SALEN–Mn complex
Pillared clays

ABSTRACT

[Mn(3,5-dtSALEN)Cl] **(I)** and [Mn(3,5-dtSALHD)Cl] **(II)** complexes (3,5-dtSALEN = *N,N′*-bis(3,5-di-tert-butylsalicylaldehyde)ethylenediamine; 3,5-dtSALHD = *N′N*-bis-(3,5-di-tert-butylsalicylaldehyde)-1,2-cyclohexanediamine) were successfully encapsulated within a natural bentonite by using three preparative approaches: **(A)** direct adsorption of every metal complex on the previously Al-pillared bentonite, Al-PILC; **(B)** two-step liquid phase methodology: (i) cationic adsorption of Mn^{2+} in Al-PILC by substituting its residual cationic exchange capacity (CEC), followed by (ii) diffusion of either 3,5-dtSALEN or 3,5-dtSALHD ligands, for in-situ generation of the corresponding interlayered metal complexes; and **(C)** simultaneous pillaring/encapsulation of the complexes on the raw starting clay. The materials were characterized by cationic exchange capacity, X-ray diffraction, atomic absorption, FT-Infrared and UV–vis spectroscopies, and N_2 adsorption at 77 K. The physical encapsulation of the complexes into final materials was proven by spectroscopic analyses. Method C yielded both highest metal incorporation and enhanced basal space on the modified clay. All materials showed to be active catalysts in cyclohexene epoxidation with hydrogen peroxide using acetonitrile as solvent (0.79 atm, 293 K). Addition of sodium bicarbonate as co-catalyst led to enhanced conversion (100%) and selectivity (70%) towards the epoxide in the presence of such a kind of heterogeneized metal-complex catalysts. The catalysts were stable and reusable along at least two catalytic cycles.

1. Introduction

Epoxidations are a class of reactions deserving of great interest since they lead to valuable and versatile intermediates for development of pharmaceutical active compounds [1], fine chemicals, polymers and paints [2–5], among others. Hydrogen peroxide constitutes an environmental-friendly and clean oxidizing agent for this kind of reactions, since it only forms water as by-product, and by its low price and wide availability [1]; however, its use in this reaction has been recognized to be complicated because of its inmiscibility in organic solvents [6]. Mn(III) complexes with Schiff-base ligands displaying coordination environment N_2O_2, also so-called SALEN complexes, have been widely reported as soluble and efficient catalysts in olefin epoxidations [7–10].

By this reason, effective immobilization of this type of active agents on solid surfaces shows several advantages, including simpler handling and separation of the products, easy recovery of the solid catalyst from the reaction mixture and lower amount of residues [11,12]. A higher catalytic performance has also been evidenced for such solid catalysts in comparison to the same complexes dissolved, operating under homogeneous conditions; appropriate immobilization allows the isolation of the active centres, preventing inactive dimers of the metal complex of the type μ-oxo-Mn(IV) to be formed in the reaction mixture [13]. Thus, heterogeneization of such a type of metal complexes has received much attention in the past few years, the attachment of several

* Corresponding author. Tel.: +57 3184079325; Fax: +57 2 7313106.
E-mail address: alejandrogaleano@udenar.edu.co (L.A. Galeano).

http://dx.doi.org/10.1016/j.molcata.2016.01.034
1381-1169/

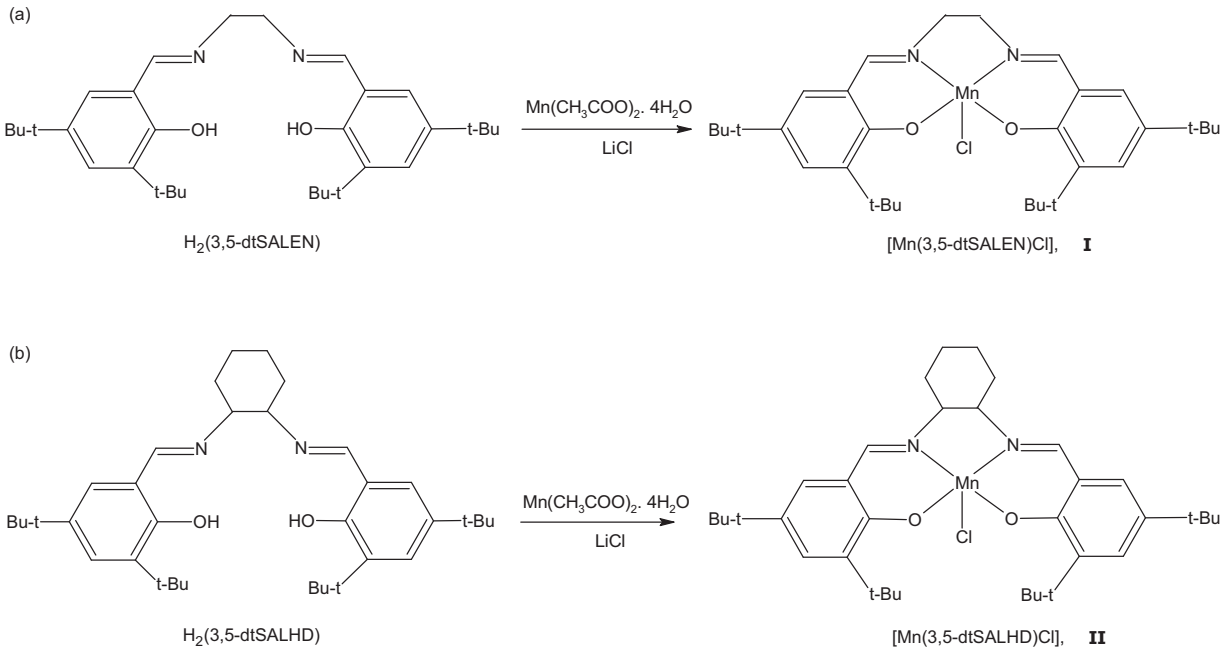

Fig. 1. General sketch employed for preparation of the SALEN–Mn(III) complexes: (a) [*N*′*N*-bis-(3,5-di-tert-butylsalicylidene)-ethylendiamine]manganese(III) chloride [Mn(3,5-dtSALEN)Cl)] **(I)** and (b) [*N*′*N*-bis-(3,5-di-tert-butylsalicylidene)-1,2-cyclohexanediamine]manganese(III) chloride [Mn(3,5-dtSALHD)Cl] **(II)**.

Mn complexes on several inorganic surfaces, like silica, mesoporous materials [14–16], activated carbon [17,18] and pillared clays [19–22] has been then reported. It is remarkable that catalysts based on pillared clays have displayed outstanding efficiency in the epoxidation of a variety of olefins [23].

Pillared clays (PILCs) are nanostructured materials very attractive to host metal complexes with catalytic activity. In general terms, these materials are prepared by exchange of the original cations present into the interlayer space of some natural clays by voluminous, highly-charged metal-polycations, mainly Al-based, that upon calcination give rise to pillars of their corresponding oxides. These interlayered species provide final materials with increased thermal stability, specific surface area and pore volume in comparison to the starting mineral [24,25]. PILCs have been successfully prepared from polycations of several metals, as Ti, Zr, Fe, and Cr, among others [26], but the clays pillared with Al (Al-PILCs) have been the most extensively studied [27]; these are prepared by employing the Keggin-like polycation $[AlO_4Al_{12}(OH)_{24}(H_2O)_{12}]^{7+}$, usually abbreviated as $[Al_{13}]^{7+}$, as interlayering species [28,29]. Therefore, the incorporation and stabilization of SALEN Mn-complexes within the interlayer of Al-PILCs may then efficiently combine in the same catalyst the high catalytic activity displayed by the metal complex with the low cost, excellent textural properties and high resistance to organic solvents featured by the Al-PILCs [13,19,20,30,31]. Various strategies have been assessed in order to confine such a family of metal complexes in clay materials, finding that the final characteristics of the resulting catalysts strongly depend on the experimental procedure used for the incorporation and stabilization of the metal complex into the clay host [19].

Using of H_2O_2 as oxidizing agent in catalytic systems where Mn is the active metal leads to competition of their decomposition products for the active centres, driving to deactivation [32]. Besides, it has been also shown that hydrogen peroxide behaves as a more effective oxidizing species in the presence of activators or co-catalysts of the reaction, like NaOH, KOH or $NaHCO_3$ [33–35]. Thus, the use of $NaHCO_3$ as co-catalyst has been reported to be crucial for achieving good conversions in the presence of Mn-based catalysts [34,36].

Accordingly and taking into account that several methods have been already tested for encapsulation of SALEN complexes in porous matrices like pillared clays, this work was focused to study the direct immobilization of two similar complexes, ([Mn(3,5dtSALEN)Cl)] and [Mn(3,5dtSALHD)Cl], having different substituents on the diimine bridge (Fig. 1) within the free channels in the interlayer space of an Al-PILC. Results may be compared to previously reported methods [19]. The effect of the structure and size of the complexes and of the insertion method on the stability and catalytic behaviour of the final functionalized materials have been evaluated in the cyclohexene epoxidation by H_2O_2 assisted by $NaHCO_3$ as co-catalyst.

2. Experimental

2.1. Materials

The preparation of the Schiff bases and their corresponding Mn(III) complexes was performed by using 1,2-cyclohexanediamine (98%), manganese chloride tetrahydrate (≥98%, ACS reagent), ethylendiamine (≥99.99%, SigmaUltra), manganese acetate tetrahydrate (≥99%), absolute ethanol (≥99.5%, ACS reagent) and *N,N*′-dimethylformamide (≥99%), all purchased from Sigma–Aldrich®, as well as 3,5-di-tert-butylsalicyladehyde (99%) from Alfa–Aesar and dichloromethane (99.9%) from Mallinckrodt. The Al-oligomeric solution used to treat the clay was prepared from $AlCl_3{\cdot}6H_2O$ (≥99%, Sigma–Aldrich) and NaOH (≥99.8% Mallinckrodt). In the catalytic experiments and the chromatographic analyses, cyclohexene (99.0%, Alfa–Aesar), cyclohexene epoxide (99.0%, Merck), hydrogen peroxide (30% w/w AR, Panreac), acetonitrile (99.0%, Aldrich Chemical), sodium bicarbonate (99.0%, Carlo Erba) and *n*-decane (≥ 99.0%, Alfa–Aesar) were used. All reagents were employed as received.

The preparation of the catalysts was made using as starting material a natural bentonite from Valle del Cauca, Colombia, (BVC). Its physicochemical and mineralogical features have been extensively reported elsewhere [37]: cationic exchange capacity, CEC = 89 meq/100 g clay dry basis; elemental composition (w/w%): SiO_2, 60.5; Al_2O_3, 24.7; Fe_2O_3, 10.2; MnO, 0.05; MgO, 3.07; CaO,

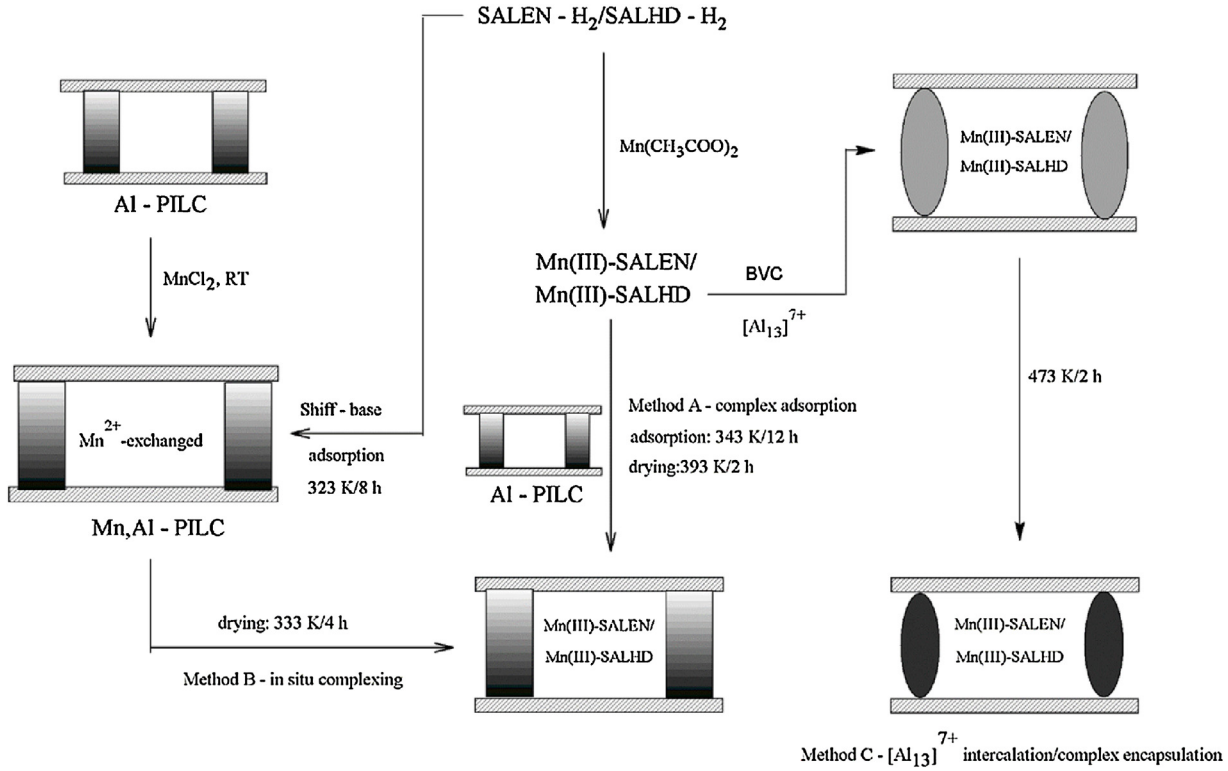

Fig. 2. Methods used to incorporate/stabilize complexes **(I)** or **(II)** between the layers of the Al-PILC: method A: direct adsorption of the metal complex on the pillared clay; method B: in-situ growing of the interlayered complex upon adsorption of SALEN/SALHD ligand on the previously Mn^{2+}-exchanged pillared clay; and method C: simultaneous intercalation of Al_{13} and encapsulation of the complex on the starting clay.

0.64; Na_2O, 0.20 and K_2O, 0.58. The pillaring process was performed on the fraction of the mineral with particle diameter (d_p) ≤ 2 μm, obtained by differential sedimentation from a water suspension of the raw clay mineral.

2.2. Synthesis of Schiff bases and Mn(III)-complexes

Schiff base ligands and their corresponding complexes [*N′N*-bis-(3,5-di-tert-butylsalicylidene)-ethylendiamine]manganese(III) chloride [Mn(3,5-dtSALEN)Cl)] **(I)** and [*N′N*-bis-(3,5-di-tert-butylsalicylidene)-1,2-cyclohexanediamine]manganese(III) chloride [Mn(3,5-dtSALHD)Cl] **(II)** were prepared adopting a methodology widely reported in the literature [13,19,38–40]. The ligands were prepared by condensation of 3,5-di-tert-butylsalicylaldehyde with the corresponding diamine (either, ethylenediamine or 1,2-cyclohexanediamine) in a molar ratio 1:2 in ethanol. Complexes (I) and (II) were obtained then by adding a saturated solution prepared with 3.66 mmol of manganese acetate in absolute ethanol to 1.83 mmol of the corresponding ligand dissolved in 25 cm^3 of the same solvent pre-heated at 353 K under reflux; air was slowly and shortly (10–20 s) bubbled through the reacting mixture since long oxidation might lead to form oxo-Mn(V) species easily detected by darkening of the brownish solution [41], which inactivate the catalytic response of the complexes in the targeted reaction. Then, the air stream was stopped and the heating was kept along one extra hour with darkening of the yellow–orange solution to brown. Afterwards, 5.29 mmol of lithium chloride in ethanol were added to achieve the access of Cl into the coordination sphere of the transition metal, and the mixture was heated further 30 min. The resulting solid was then dissolved in dichloromethane and refined employing the method from Cubillos et al. [40] by means of liquid extraction with *n*-heptane. The final solid was recovered by vacuum filtering and then dried at room temperature in a desiccator. The same procedure was used to prepare both complexes.

2.3. Preparation of the Al-pillared clay

A standard procedure previously reported was used [42]. The pillaring precursor $[Al_{13}]^{7+}$ was prepared by very slow dropping of aqueous NaOH 0.2 mol/dm^3 on $AlCl_3{\cdot}6H_2O$ 0.2 mol/dm^3, to get a final ratio OH^-/Al^{3+} = 2.4 (final pH around 4.3). Such a resulting oligomeric solution was then added on a water suspension of the clay until final nominal loading with 20 mmol Al^{3+}/g clay. The aluminosilicate thereby interlayered was then washed in a dialysis tubing cellulose membrane (Sigma) along four cycles with distilled water, dried at 333 K and then heated in air, at 673 K for 2 h, to give rise to the Al-pillared clay (Al-PILC).

2.4. Incorporation and stabilization of the Mn(III) complexes on Al-PILC

Every SALEN–Mn(III) complex was encapsulated in Al-PILC by means of three approaches reported elsewhere [19], summarized in Fig. 2. The ratio used was always 0.5 mmol complex/g clay.

2.4.1. Method A—direct adsorption of the complex on the Al-pillared clay

A solution of the complex in *N,N′*-dimethylformamide (1.0×10^{-3} mol/dm^3) was poured on Al-PILC clay and the mixture heated to reflux (343 K) throughout 12 h under gentle stirring. The solid was then separated by filtration, washed by centrifugation using ethanol and then distilled water, pre-dried at 333 K and finally heated at 393 K for 2 h until final dry state. The so prepared materials were denoted as (IA)Al-PILC and (IIA)Al-PILC for complexes (I) and (II), respectively.

2.4.2. Method B—in-situ growing of the complex by adsorption of the Schiff-base on the Al-pillared clay previously exchanged with Mn^{2+}

The Al-PILC was treated with a 2.0 mol/dm^3 aqueous solution of $MnCl_2{\cdot}4H_2O$ under stirring for 8 h, in order to obtain the Mn^{2+}-exchanged form of the Al-pillared clay by cation exchange; the incorporated Mn content is denoted as $Mn_{incorporated}$. The supernatant was retired and the procedure was entirely repeated once again. Then, the solid was washed by centrifugation with distilled water along four cycles and dried at 333 K (Mn,Al-PILC). Afterwards, a 0.01 mol/dm^3 solution of the Schiff-base in methanol was added on a suspension of the solid (1 g Mn,Al-PILC/100 cm^3 methanol) in proper amount for a final ratio $Mn_{incorporated}$:ligand = 1:1 (equivalent to a ratio 0.6125 mmol ligand/g Mn,Al-PILC), and the mixture was then refluxed at 323 K for 8 h with stirring. The materials were washed with dichloromethane by centrifugation to retire the excess of either ligand or complex deposited on the external surface of the clay, and finally dried at 333 K, giving rise to (IB)Al-PILC and (IIB)Al-PILC materials for the immobilized complexes (I) and (II), respectively.

2.4.3. Method C—simultaneous $[Al_{13}]^{7+}$-intercalation/complex-encapsulation on the starting clay

An ethanolic solution of the complex (2 mmol of complex/dm^3) was slowly poured on the $[Al_{13}]^{7+}$ oligomeric solution, reaching the ratios employed above: 20 mmol Al^{3+}/g clay and 0.5 mmol complex/g clay. The resulting mixed solution was slowly dropped under strong shaking on a suspension of the clay previously swollen for 24 h in water (2.0% w/v) at room temperature. The resulting suspension was stirred for 1 h and then allowed to stand for 2 h. The solid was recovered by centrifugation, washed with distilled water until final conductivity close to 10 μS/cm, and the excess of the complex removed by two sequential cycles of Soxhlet extraction, the first cycle with ethanol and the second one with dichloromethane, until no detection of the complex in the liquid phase. The final solid was dried at 333 K and heated at 473 K for 2 h from room temperature, under a heating rate of 1 K/min. Solids were denoted as (IC)Al-PILC and (IIC)Al-PILC for complexes (I) and (II), respectively.

2.5. Physicochemical characterization of catalysts

The 200–700 nm UV–vis spectra of the Schiff-bases and their corresponding Mn(III) complexes were recorded in a Merck UV–vis Pharo 300 spectrophotometer on dichlorometane 1.0 mmol/dm^3 solutions. The 400–4000 cm^{-1} FT-IR spectra were obtained from pellets of every sample in KBr (spectral grade, Sigma–Aldrich) in a Thermo Scientific Nicolet FTIR-6700 spectrophotometer with resolution of 4 cm^{-1}, from average of 32 scans. ^{1}H NMR spectra of the ligands in $CDCl_3$ were made in a 400 MHz Bruker Ultrashield™ apparatus.

The content of Mn in the solids was determined by atomic absorption spectroscopy (AAS) in a PerkinElmer 2380 spectrometer on the samples previously digested in a HF/HNO_3 mixture. The cationic exchange capacity, CEC, of the clay materials was measured by extensive exchange with 2.0 mol/dm^3 ammonium acetate followed by several cycles of distilled water washings, drying (333 K) and micro-Kjeldahl determination of the $NH_{3(g)}$ released from the $(NH_4)^+$-exchanged solids. The XRD patterns were recorded on powdered samples in the range of 2–15° 2θ at 2° 2θ/min in a Siemens D-500 Diffractometer, using Ni-filtered Cu Kα (λ = 1.5405 Å) incident radiation. Specific surface area of the solid materials was determined at 77 K in a Quantachrome CHEMBET 3000 equipment; the samples were degassed at 463 K for 2.5 h under a He/N_2 70/30 stream. Specific surface area were calculated using the BET equation (S_{BET}).

2.6. Catalytic experiments

The experiments of the cyclohexene epoxidation were performed using hydrogen peroxide as oxidizing agent in a glass, jacketed-batch-reactor open to the atmosphere, at room conditions (0.79 atm and 293 K in average). In a general experiment, the reactor was charged with 3.0 cm^3 of acetonitrile, 1 mmol of cyclohexene, 1 mmol of sodium bicarbonate and 0.02 g catalyst. Dropping of 4–12 mmol of H_2O_2 was performed along 5 h of reaction under constant flow rate and stirring, while samples of 0.1 cm^3 were taken every hour until 8 h as final time of reaction. Each sample was microfiltered (Hydrophobic PTFE, 0.45 μm) and then analysed by gas chromatography in a Shimadzu GC-14A device equipped with a FID detector and a Varian VF-1 (15 m × 0.25 × 0.25 μm) capillary column, using the following program: the temperature of the column started and was kept at 60 °C for 4 min, then raised to 80 °C (5 °C/min), 4 min, then until 120 °C (5 °C/min), 1 min, 150 °C (20 °C/min), 1 min, and finally to 250 °C (20 °C/min) during 1 min. Calibration curves were built in advance for cyclohexene and cyclohexene oxide. The response factors were determined by using the areas below every peak. Therefore, the concentrations of reactant and the targeted product were calculated by extrapolation of the signal of FID detector within the corresponding calibration curve. Every run was made using a gradient of temperature between 333 and 523 K throughout 29 min, where the temperature of both the injector and the detector was maintained at 523 K. For assessment of the catalyst's reusability, the solid was recovered from the reaction mixture, washed twice with acetonitrile and then five times with methanol in order to remove any remaining reactant or product; every catalyst was then reused in the cyclohexene epoxidation under identical experimental set-up.

3. Results and discussion

3.1. Characterization of Schiff-base ligands and their Mn(III)-complexes

The SALEN-like ligands and derived Mn(III)-complexes were characterized by UV–vis, FTIR and NMR spectroscopies. The UV–vis spectra (CH_2Cl_2) showed characteristic signals in λ_{max} 280 nm and around 330 nm corresponding to M–L charge transfer transitions $n \rightarrow \pi^*$ and $\pi \rightarrow \pi^*$, respectively, the last one due to the presence of the imino group (—C=N) [18]. Besides, both complexes (CH_2Cl_2) showed a signal with λ_{max} close to 430 nm, that could be also attributed to M–L charge transfer, as well as other very weak signal around 500 nm due to a *d–d* transition characteristic in d^4 manganese ions [38]. The FTIR spectra of ligands and complexes displayed the expected characteristic signals for this kind of compounds. Both ligands H_2(3,5dtSALEN) and H_2(3,5-dtSALHD) showed, respectively, the following (ν_{max}/cm^{-1}): 3438–3432 (OH, ν); 2995–2990 (=C—H, ν); 1595–1594 (C=C, ν); 2962–2961 (—CH_3, ν_{as}); 2869–2863 (—CH_3, ν_s), and 1629–1630 (—N=C, ν), the last signal proving the formation of the imine bridge. Both complexes showed the same signals exhibited by the ligands; however, the signal of the imine is particularly useful since it became shifted to lower wavenumbers, 1611 and 1608 cm^{-1} for complexes (I) and (II) respectively, in comparison with their corresponding ligands, evidencing the formation of the organometallic adducts. The signals at 567–546 (Mn–O, ν) and 489–485 (Mn–N, ν) are featured by the linkage between the metal and the N_2O_2 coordination sphere. The characterization of the ligands by NMR revealed the following; (i) H_2(3,5-dtSALEN) ^{1}H NMR (δ ppm): 13.66 (s, 2 H, OH), 8.42 (s, 2 H, CH=N), 7.40 (d, 2 H, ArH), 7.10 (d, 2 H, ArH), 3.95 (m, 2 H, C=NCH), 1.47 (s, 18 H, *t*-butyl). (ii) H_2(3,5-dtSALHD) ^{1}H NMR (δ ppm): 13.72 (s, 2 H, OH), 8.32 (s, 2 H, CH=N), 7.33 (d, 2 H, ArH), 7.01 (d, 2 H,

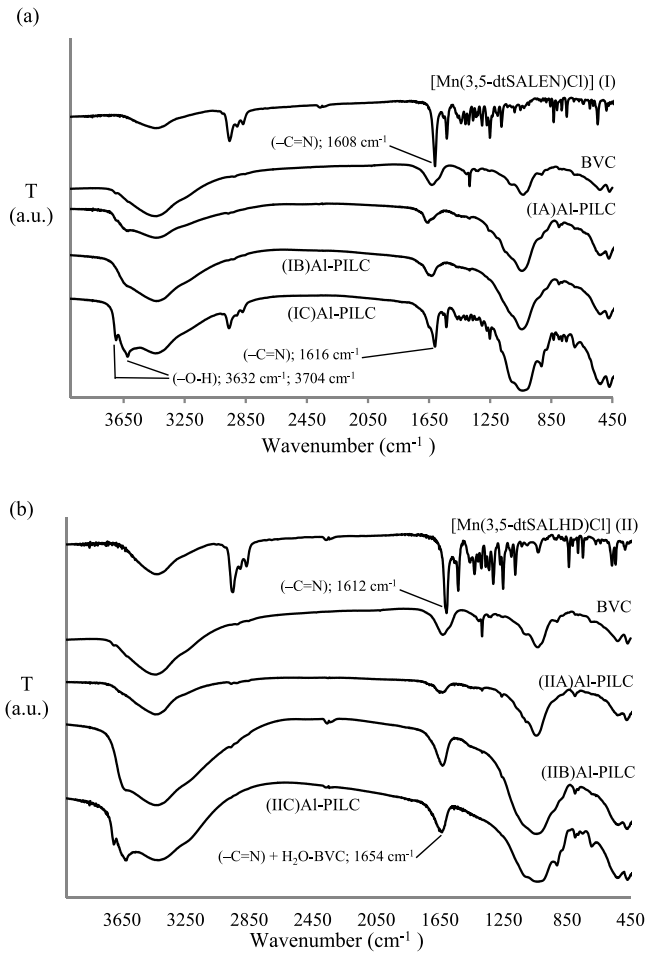

Fig. 3. FTIR spectra of the Mn-complexes and their clay-derived solids: (a) [Mn(3,5-dtSALEN)Cl)] **(I)** and (b) [Mn(3,5-dtSALHD)Cl] **(II)** complexes by every method of preparation.

ArH), 3.35 (m, 2 H, C=NCH), 1.91–1.56 (m, 8 H, cyclohexyl-H), 1.44 (s, 18 H, *t*-butyl). Thus, it was confirmed that the targeted ligands and complexes were successfully prepared.

3.2. Characterization of the solid, immobilized Mn(III)–SALEN catalysts

The FTIR spectra of the materials are compared in Fig. 3. The typical signals of the aluminosilicate together with those from the Mn-complexes are observed. First of all, the intense and broad band in the region 3700–3300 cm^{-1}, that can be assigned to the —OH stretching in Al—OH and Si—OH groups of the starting clay [13], remained for the immobilized complexes obtained by the three methods, suggesting that no covalent interaction was established with the metal centre of the SALEN-complexes, i.e. that mainly physical encapsulation took place. The solids derived from method C for both metal-complexes clearly displayed stronger signals; that is somewhat expectable since the final solids were calcined at lower temperature than their counterparts of the methods A and B (473 K vs. 673 K), and a higher fraction of surface hydroxyls remains in the solids. This band exhibits a couple of shoulders in the edge of higher frequency (ca. 3632 cm^{-1}), that may be related to the hydroxyl groups from the Al-pillars. On the other hand, the immobilization of both Mn(III)-complexes was evidenced by the shifting of the imine group signal (—C=N), observed at 1690–1640 cm^{-1} for both ligands and appearing at lower frequency (1620–1600 cm^{-1}) for the corresponding complexes, and being observed for (IC)Al-PILC solid at 1616 cm^{-1} (the other solids showed a broad peak between 1680 and 1650 cm^{-1}, in which this signal may probably be overlapped with the bending of adsorbed water, observed in the starting clay at 1638 cm^{-1}). This suggests that A and B methods promoted covalent interactions of the complexes with the hosting inorganic matrix, due in part to the higher temperature of the treatment. In the same sense, the antisymmetric stretching from tetrahedral SiO_2 in smectites, observed at 1032 cm^{-1} for BVC solid, shifted to higher frequencies, in the range 1060–1100 cm^{-1}, in all the modified solids, also suggesting host-guest interactions of the complexes with the clay. In addition, a set of bands can be seen in the 1500–1200 cm^{-1} region, similar to those displayed by the free complexes in this region. Finally, Mn—O and Mn—N stretchings, expected at wavenumbers near to 575 cm^{-1} and 492 cm^{-1}, respectively, unfortunately overlapped with the strong Mg—O stretching of the clay, avoiding the use of these key signals from SALEN for evaluating the successful immobilization of the complexes inside the inorganic matrix.

Moreover, the solid (IC)Al-PILC shows not only the more intense bands in comparison to the other two immobilization methods, but also the imine group signal (ca. 1616 cm^{-1}) closer to that of the free [Mn(3,5-dtSALEN)Cl)] complex; indeed, it is noteworthy for the same material the presence of strong signals at 2900–2800 cm^{-1} corresponding to C—H stretching of the methyl groups from the *t*-butyl substituents. All these observations, together with its higher efficiency in the Mn uptake (see $Mn_{(IE)}$ in Table 1), strongly suggest that method C was the best procedure to successfully attach the complex to the aluminosilicate without significant modification of its molecular structure.

Mn contents in the modified materials showed insertion efficiencies between 60 and 90% (Table 1). Besides, the content of Al increased in comparison to the starting clay because of the incorporation of the alumina pillars, causing a parallel decrease in Mg, Si and Ca contents.

It is worth noting that methods B and C displayed higher insertion percentages than method A. The lower incorporation efficiencies for method A could be due to the easier leaching of the complexes from the solids during the washing steps, as this method leads to the complexes mainly incorporated on the external surface of the solids. The high insertion of Mn in (IB)Al-PILC and (IIB)Al-PILC solids indicates that Mn homoionization of the Al-pillared clay before the treatment with the ligands favoured the metal uptake and stabilization in the clay matrix; as confirmed by the higher compensation of CEC observed for the solids prepared using method B (C_{CEC} in Table 1). Finally, solids obtained from method C displayed the highest Mn contents, probably because under simultaneous pillaring and encapsulation the complexes underwent easier access into the porous hosts.

The CEC values demonstrated that a compensation of the CEC of the clay by Al_{13} pillars was achieved in all the modified materials. Moreover, it must be also accounted that solids obtained by method A showed very similar C_{CEC} values that Al-PILC, whereas materials modified by either methods B or C displayed significantly higher values. It may be inferred that B and C methods allowed the complexes to get immobilized mostly into the interlayer space of the clay mineral, thus contributing to further compensation of the starting CEC. Regarding the nature of the complex, materials modified with complex II showed higher efficiency in the Mn uptake and higher CEC compensation than those modified with complex I, except for method C. This was probably due to the presence of a voluminous substituent near the imine bridge of II. In spite of the bigger size of complex II respect to complex I, the adsorption of the complex (method A) or of the ligand (method B) of system II was apparently more efficient in terms of Mn uptake, under very similar values of compensation of the initial CEC. This suggested

Table 1
Elemental composition (% w/w)[a], compensation of the initial cation exchange capacity (C_{CEC}), BET specific surface area (S_{BET}), and basal spacing (d_{001}) for the starting clay, the Al-pillared clay and the Mn-complex-functionalized solids.

Sample	Fe_2O_3	CaO	MgO	SiO_2	K_2O	Al_2O_3	Mn	$Mn_{(IE)}$[b] (%)	C_{CEC}[c] (%)	S_{BET} (m^2/g)	d_{001}[d] (nm)
BVC	4.19	0.21	0.58	57.3	0.14	7.16	0.03	–	–	80	1.42
Al-PILC	1.79	0.04	0.58	49.0	0.05	9.18	0.04	–	34	208	1.70
(IA)Al-PILC	3.36	0.04	0.45	44.8	0.10	10.2	1.89	68.8	36	50	1.59
(IB)Al-PILC	3.50	0.03	0.35	53.3	0.07	11.3	2.40	87.4	56	65	1.65
(IC)Al-PILC	4.19	0.03	0.18	51.1	0.14	12.8	2.52	91.7	56	73	2.76
(IIA)Al-PILC	3.95	0.04	0.75	49.8	0.24	13.1	2.11	76.8	37	38	1.70
(IIB)Al-PILC	4.53	0.03	0.35	47.3	0.11	13.3	2.53	92.1	59	16	1.71
(IIC)Al-PILC	4.07	0.03	0.58	41.9	0.20	13.8	2.22	80.8	55	55	1.90

[a] The metal contents are expressed in terms of their corresponding most stable oxides; except Mn, which is expressed as element content since it is retained on the clay in its complex form. All values are dry-basis.
[b] $Mn_{(IE)}$: insertion efficiency of Mn.
[c] C_{CEC} = percentage of the CEC of the starting clay that was compensated by the sequential Al-pillaring and Mn-complex immobilization treatments.
[d] Determined from the corresponding powder XRD patterns.

that adverse adsorption of complex II into the micropores of the pillared clay was overcome by an extra stability provided to the complex by the cyclohexane substituent on the diimine bridge, but this bigger size is apparently not determinant on the stabilization within the interlayer space of bentonite, since the complexes are featured by a planar structure that fits well into the quasi-infinite two dimensional interlayer space available in Al-PILC, only limited by the average distance between the alumina pillars. However, somewhat unexpectedly, the method C, in which the Al_{13} intercalation and complexes encapsulation were simultaneous, showed lower Mn uptake, although similar CEC compensation for complex II respect to complex I.

The BET specific surface areas of the materials are also summarized in Table 1; S_{BET} decreased for the heterogeneized complexes compared to the Al-pillared clay Al-PILC. This can be attributed to the insertion of the complexes within the porous network of the pillared aluminosilicate provoking a partial blockage of the pores. Besides, the catalysts displaying lower specific surface area are those prepared with complex II, which has the voluminous cyclohexyl substituent on the diimine bridge, in according with the effect reported elsewhere [43]. In general, the materials prepared by method C undergone lower decreases in the specific surface area upon complex immobilization. In addition, as somehow expectable, the larger size of the SALEN ligand decreased in higher amount the final specific surface area of the catalysts prepared using method B, in which the *in-situ* formation of the complexes by diffusion of the ligand through the clay pores up to the previously exchanged Mn^{2+} cations is obviously more sterically hindered in the case of complex II.

The XRD powder patterns for the starting clay and the materials modified with complex I (a) and complex II (b) are compared in Fig. 4, and their corresponding basal spacings are given in Table 1. All the modified solids displayed a shifted d_{001} signal respect to the starting mineral (6.20° 2θ, 1.42 nm), showing that the three methods allowed to incorporate the SALEN complexes without loss of the expanded structure of the pillared clay. The solids prepared by methods A y B, in which the immobilization was performed on the clay previously pillared, basal spacings (1.59–1.71 nm) were pretty similar to that of the pillared bentonite Al-PILC (1.70 nm); hence, the incorporation of Mn did not significantly decrease the basal spacing of the precursor solids, in agreement with the behaviour reported by Cardoso et al. [19]. However, the broadening of the d_{001} peaks in the complex-functionalized solids evidenced a loss of *c*-axis ordering, suggesting a heterogeneous distribution of the Mn-complexes and the alumina pillars, although without drastically affecting the thermal stability of the solids.

The solids prepared using method C displayed basal spacings (1.90 nm–2.76 nm) clearly higher than Al-PILC. The presence of the complex in the system apparently led to enhanced, widespread

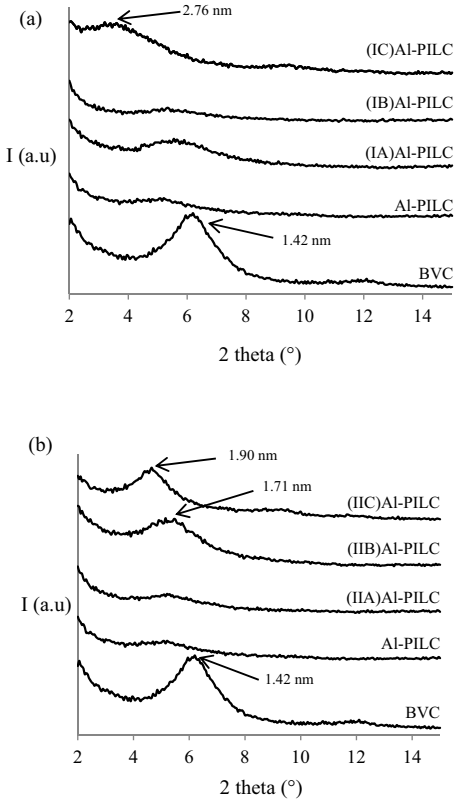

Fig. 4. Small-angle powder XRD patterns of the starting and modified materials: (a) complex **(I)**—derived catalysts and (b) complex **(II)**—derived catalysts.

distribution of the pillars within the interlayer space of the clay, taking into account that method C involved simultaneous intercalation/encapsulation of the SALEN complexes. At the same time, the basal spacing of (IC)Al-PILC with the smallest Schiff-base ligand, was clearly higher than that of (IIC)Al-PILC; suggesting a very interesting role of the SALEN-like complexes in the intercalation of the clay with the Al-polycations. Apparently, complex I induced a swelling of the clay layers in the presence of the pillaring polycations significantly higher than the typical values reported for the Keggin adduct, around 0.7–0.9 nm, as measured before or after the final thermal treatment, to more than twice that value (~1.8 nm). Furthermore, although solid (IIC)Al-PILC displayed the higher basal spacing in between the set of materials prepared with complex II (1.9 nm), this effect was not so important as in the case of (IC)Al-PILC. While complex II promoted a more homogeneous distribution of the pillaring species throughout the interlayer of the clay by

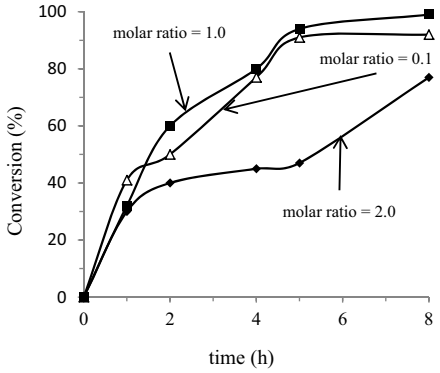

Fig. 5. Effect of the $NaHCO_3$/cyclohexene molar ratio on the conversion of cyclohexene by H_2O_2 in the presence of (IC)Al-PILC catalyst.

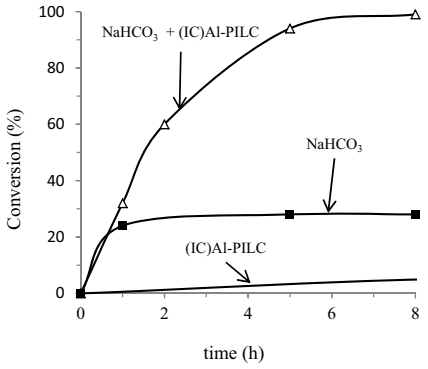

Fig. 6. Catalytic performance of the bicarbonate-assisted cyclohexene epoxidation in the presence or absence of (IC)Al-PILC catalyst.

serving as a kind of organometallic spacer, complex I seemed to intervene in the aggregation of the Keggin-like species probably leading them to form dimers by self-assembly around the Mn-complex or inducing larger polynuclear species of the metal before and even during the intercalation stage [44].

3.3. Bicarbonate-assisted cyclohexene epoxidation by H_2O_2

The effect of the amount of bicarbonate used as co-catalysts was first investigated by carrying out a series of experiments using (IC)Al-PILC as catalyst and adding various amounts of $NaHCO_3$ (see Fig. 5). The increase from 0.1 to 1.0 in the bicarbonate/cyclohexene molar ratio led to enhance the final cyclohexene conversion from 92 to 99% after 8 h of reaction, with similar trends at lower times. Moreover, further increase in the $NaHCO_3$ amount, up to twice the substrate, caused the opposite effect, decreasing the conversion at 8 h of reaction as well as making slower the rate of reaction for times higher than 1 h.

Some reports, like that from Yao and Richardson [45], have demonstrated that bicarbonate is a good activator of H_2O_2 in aqueous catalytic epoxidations of alkenes, in terms of allowing higher conversions, while decreasing the parasite disproportionation. Therefore, the use of bicarbonate as co-catalyst has shown to be crucial in order to achieve maximum olefin conversion in the presence of Mn–SALEN complexes at lower times of reaction. Lane et al. [34] proposed that a key factor to get high conversions in bicarbonate-assisted olefin epoxidations with H_2O_2 is the formation of the peroxymonocarbonate ion $(HCO_4)^-$, a nucleophile more reactive than hydrogen peroxide, formed in the pH range between 7.0 and 9.0. Therefore, the result observed can be explained considering that peroxymonocarbonate ion is effectively stabilized at bicarbonate/cyclohexene molar ratio of 1.0, but for ratios significantly exceeding this value (as in the case of 2.0), the pH may surpass 9.0, the deprotonation and decomposition of HCO_4^- to CO_3^{2-} become significant according to the equilibrium in Eq. (1), strongly decreasing the concentration of HCO_4^- and affecting the conversion of the olefin.

$$HCO_3^- + H_2O_2 \rightleftharpoons HCO_4^- + H_2O \quad (1)$$

Afterwards, some experiments were made with or without the addition of catalyst to point out the role truly played by this and the bicarbonate ion in the olefin conversion (Fig. 6). $NaHCO_3$ even in the absence of the catalyst was capable to contribute to the conversion of cyclohexene (though below 30%, 8 h), showing that the peroxymonocarbonate ion is itself active, although fairly less efficient when the (IC)Al-PILC catalyst is present (99%, 8 h). In the presence of the same complex-immobilized clay catalyst but without addition of bicarbonate co-catalyst, a more rather negligible conversion was achieved (around 6.0%) upon 8 h of reaction. This demonstrates the key role played by $NaHCO_3$ for the activation of H_2O_2 as oxidizing agent in epoxidation, reported mainly to be related with the enhanced rate of the epoxidation against the parasite disproportionation of the hydrogen peroxide [34]. It is obvious that the combination of various properties as the formation of the active peroxymonocarbonate species, the catalytic activity of the Mn(III)–SALEN complex and the stability and encapsulation efficiency of the hosting pillared clay allowed to obtain improved catalytic performance, avoiding at the same time the full leaching of the complex from the solid and preventing the formation of inactive species. Other series of catalytic experiments showed the effect of the molar ratio H_2O_2/cyclohexene in the conversion of the olefin, using (IC)Al-PILC keeping constant the amounts of catalyst and bicarbonate (0.02 g and 1 mmol, respectively) (Table 2). Using a molar ratio of 4.0, no conversion at all was found, but when the molar ratio was 10 conversion achieved was 99%. A further increase in the molar ratio to 12 did not conduce to any further improvement of the cyclohexene conversion, so it can inferred that a ratio H_2O_2/cyclohexene between 4 and 10 allows to dramatically enhance the olefin conversion in the presence of the Mn–SALEN immobilized clay-catalysts; although a higher concentration of peroxide may lead to the formation of other products of the cyclohexene oxidation contributing to increase the olefin conversion [36], the disproportionation of hydrogen peroxide also forms higher amounts of water, decreasing the overall efficiency of the oxidizing agent. The global efficiency of conventional catalytic epoxidations is often affected by the presence of water. It happens mainly by the ring opening of the epoxides by water catalysed by Lewis acid-sites [34]. However, in our case it must be realized that two phases with very different polarity are into the same reacting mixture, where the epoxide of course is favoured in the organic phase (acetonitrile) [46]. Therefore, one of the main advantages of the bicarbonate-assisted epoxidations by H_2O_2 is in fact the lower susceptibility of the system to the presence of water. It occurs thanks to the buffer effect exerted by the bicarbonate, where the slightly basic pH promotes formation of the peroxymonocarbonate species useful enhancing the rate of epoxidation, while the ring opening of the epoxides towards the undesired diol

Table 2
Cyclohexene conversion as a function of the H_2O_2/cyclohexene molar ratio in the presence of the Mn–SALEN clay catalyst (IC)Al-PILC.

Molar ratio H_2O_2/cyclohexene [a]	Cyclohexene conversion (%)	H_2O_2 efficiency [b] (%)
4	0	0.0
10	99	9.9
12	99	8.2

[a] Catalyst loading = 0.02 g; $NaHCO_3$ loading = 1.0 mmol.
[b] Calculated as follows: H_2O_2 efficiency (%) = (mmol of H_2O_2 reacted for cyclohexene conversion/mmol of H_2O_2 added) × 100.

Table 3
Cyclohexene epoxidation catalysed by SALEN- and SALHD- Mn(III) complexes immobilized on the Al-pillared bentonite.

Catalyst	Run	Conversion [a] (%)	Selectivity [b](%)	Yield [c] (%)	H_2O_2 efficiency [d](%)	TON [e]
(IA)Al-PILC	First	99	63	62	9.9	90
(IB)Al-PILC	First	99	63	62	9.9	71
(IC)Al-PILC	First	99	70	69	9.9	75
	Second	85	ND	ND	8.5	ND
(IIA)Al-PILC	First	96	30	29	9.6	38
(IIB)Al-PILC	First	97	26	25	9.7	27
(IIC)Al-PILC	First	100	77	77	10.0	95
	Second	84	ND	ND	8.4	ND

[a] Determined by GC-FID; time of reaction = 8 h. ND—not determined.
[b] Determined as follows: selectivity (%) = (mmol epoxide/mmol cyclohexene reacted) × 100.
[c] Yields were calculated as the product (conversion × selectivity) divided by 100 in each case.
[d] Calculated as follows: H_2O_2 efficiency (%) = (mmol of H_2O_2 reacted for cyclohexene conversion/mmol of H_2O_2 added) × 100.
[e] TON = (mmol cyclohexene epoxide/mmol Mn in the catalyst).

becomes inhibited in absence of the Lewis acid-sites. Besides, it can be inferred that the equilibrium of Eq. (1) contributes to decrease the fraction of the H_2O_2 decomposed via disproportionation, in other words, to increase the efficiency of the H_2O_2 in the reaction. Moreover, the obtained hydrogen peroxide efficiencies were low due to the theoretical relationship of 1 mol of hydrogen peroxide required to epoxidize 1 mol of cyclohexene (Tables 2 and 3). However, it must be also remarked that our results displayed efficiencies in close correlation with other studies carried out also in aqueous medium and with hydrogen peroxide as oxidizing agent, as the results reported by Lane et al. [34], who found that the bicarbonate-assisted epoxidation by hydrogen peroxide of a number of olefins, including cyclohexene, required 10 equivalents of this oxidizing agent for the full conversion of the olefin. As it can be seen, all of our catalysts showed cyclohexene conversions between 96 and 100% when used with a molar ratio H_2O_2/cyclohexene = 10 (Table 3). Furthermore, Costa et al. [49] more recently reported conversions ranging between 11.8 and 25.8%, but using a significantly lower ratio H_2O_2/cyclohexene = 1.2. Remarkably, no bicarbonate co-catalyst was used at all.

The high conversions here reported have been found in several olefin's epoxidations, but mostly performed in the presence of organic oxidizing agents like iodosylbenzene or meta-chloroperoxybenzoic acid [19,47], in order to achieve proper miscibility in the organic mixtures. Also because the presence of water, a product of the disproportionation of H_2O_2, promotes the decomposition of the epoxide decreasing the selectivity. Recently, it was also attained a 50% styrene conversion by using hydrogen peroxide in acetonitrile as solvent, but a ratio H_2O_2/styrene of 5.0 was required and this value was enhanced when the reaction was carried out in more polar solvents [48]. Before, Costa et al. [49] obtained increasing cyclohexene conversions in the range of 20–26% in the epoxidation with H_2O_2 catalysed by Mn-, Co- or Fe-metalloporphyrins anchored on MCM-41, but using a fairly lower ratio H_2O_2/cyclohexene of 1.2. Finally, a new Mn–SALEN type complex, [Mn(saldien)(N_3)], immobilized on SBA-15 mesoporous material was recently reported catalysing cyclohexene oxidation by hydrogen peroxide with conversions of 11–38% as a function of the peroxide dosage and time of reaction [50]. In our case, H_2O_2/cyclohexene ratios exceeding 10 were needed probably to overcome not only the low miscibility in the organic mixture of reaction, but also a partial parasite degradation of the oxidizing agent in the presence of some traces of Fe in the inorganic hosting mineral; moreover, there must be remarked that most of the iron content in the starting clay here used is located within the lattice of the mineral as reported in advance [37], and then no substantial contribution of this reaction in the peroxide consumption should be expected.

The conversion, selectivity, yield and TON values displayed by all the solids are summarized in Table 3. Regarding the size of the immobilized complexes, both Mn(III)-complexes delivered almost the same close to full conversions of cyclohexene. However, in terms of both selectivity and yield the catalysts based in complex I were in general more effective (60–70%) than those of complex II (30–77%), as well as fairly less sensitive regarding the method of preparation. Moreover, the solid (IIC)Al-PILC displayed the highest catalytic performance in terms of conversion, selectivity and yield in a single catalytic run. This should be probably related to the enhanced physicochemical properties of this catalyst in terms of both basal spacing and specific surface area with respect to the counterparts obtained by methods A and B (Table 1). In addition, the enhanced selectivity demonstrated by the two solids prepared through simultaneous Al_{13}-intercalation/complex encapsulation (method C), irrespective the nature and size of the Mn–SALEN complex, suggests that this method guarantees more selective confinement and stabilization of the complex within the interlayer space of the pillared clay. Similar improvement of styrene epoxidation by iodosylbenzene using Mn(III)–SALEN immobilized on clay minerals have been reported, where the simultaneous Al_{13}-intercalation/complex encapsulation was the method with the lower leaching of the complex [19]. In other words, a considerable fraction of the complex or the ligand may remain deposited on the external surface of the hosting clay when using methods A and B, respectively, and although more easily accessible, their catalytic performance could not control the nature of the products, control more related to the shape and size of the solid porosity, and being more susceptible of leaching along the first catalytic run.

Finally, regarding the catalytic activity displayed by the clay-catalysts, the top turn-over number (TON) value was reached for (IIC)Al-PILC catalyst (95), which was slightly higher than the one reported elsewhere by Lane et al. [34], who used dissolved $MnSO_4$ as active species. This clearly shows that our catalysts did not undergo loss of activity by the immobilization on the solid phase but they were a little bit more active than the metal ions. This probably obeyed to intrinsic higher activity of the immobilized Schiff–Mn(III) complexes, as well as the promoting effect provided by the clay-catalytic support. In a similar way, Fraile et al. [51] reported catalytic activity for Mn–SALEN complex [*N*′*N*-bis-salicylidene-ethylendiamine]manganese(III) chloride, supported on several clays. In the case of the commercial bentonites, the TON numbers were significantly lower than ours (6.2 and 12.8, for direct exchange or metal exchange followed by treatment with the ligand, respectively), probably suggesting that simultaneous intercalation/complex-encapsulation employed in this work seriously improved the catalytic response of the SALEN-like complex. Finally, Costa et al. [49] obtained much higher TON values using a Mn–porphyrin complex immobilized on MCM-41 (1.54×10^5). Such a significant difference could be of course explained by a higher intrinsic activity of the Mn–porphyrin, but it must also be accounted that these authors calculated the TON number based on

the yield of all products and not only to the desired epoxide. In addition, as long as a pretty lower molar ratio H_2O_2/cyclohexene = 1.2 was used, a higher probability of the molecules of the oxidizing agent to be activated by a metal centre is expectable, before direct attack on the olefin or the parasite reaction of the peroxide disproportionation to take place, improving overall catalytic activity.

This coincides with previous studies using hybrid catalysts of the Mn(III)–SALEN type stabilized on pillared clays by a similar strategy, where high olefin conversions and good selectivities toward the epoxide were also achieved, using iodosylbenzene as oxidizing agent [19].

Another factor probably related to the increased selectivity displayed by (IIC)Al-PILC catalyst with respect to (IC)Al-PILC would be the higher steric hindrance exerted by the voluminous cyclohexane ring on the diimine bridge [13]. This suggests that not only the preparative strategy but also the size of the substituents on the diimine ligand bridge may strongly control the overall catalytic performance of the SALEN–Mn(III)/Al-pillared clay catalysts in olefin epoxidations. It has been widely stated that the activity and selectivity in asymmetric synthesis of epoxides are strongly affected by the way the olefin approaches the catalytic centre and then, in heterogeneized complexes, the orientation at which it becomes stabilized within the solid matrix plays an important role on the enantiomeric selectivity [52]. However, in our case the selectivity was assessed in terms of the fraction of the olefin finally converted to the desired epoxide in either optical form. Hence, selectivity is mainly governed by the pathway either, homolytic or heterolytic, the hydrogen peroxide decomposition follows in the presence of the catalyst and the co-catalyst. It is well known that the heterolytic pathway leads to increased incidence of side-products than the homolytic one. Although the homolytic route may induce the further decomposition of the epoxide by the free radicals, it has been reported that the incidence of this on the selectivity is negligible in comparison to the influence exerted by the heterolytic decomposition (disproportionation) of the peroxide [53]. In the other hand, different selectivity to the epoxide found in our results as a function of the final basal spacing displayed by the clay-catalysts (see for instance d_{001} values of (IC)Al-PILC vs (IC)Al-PILC in Table 1) can be explained in terms of bigger pore sizes and surfaces when d_{001} increases instead than different orientations displayed by the metal complexes within the framework of the functionalized pillared clay. Apparently in the case of the cyclohexene epoxidation, the selectivity to the epoxide is favoured by basal spacings as close as possible to those values typical of pillared clays (1.70–1.90 nm), probably because higher pore sizes miss shape-selectivity induced by the pore channels of the modified aluminosilicate.

The highly active catalysts ((IC)Al-PILC and (IIC)Al-PILC) were selected for reusing tests. A slight decrease in the cyclohexene conversion was observed in the second catalytic run for both catalysts (see Table 3). This showed that SALEN- and SALHD–Mn(III) complexes displayed high stability even under the aggressive oxidizing conditions of reaction when they were stabilized by simultaneous intercalation/encapsulation. It has been proposed that this type of catalysts would be employed up to four sequential runs without significant loss in their catalytic properties [13,19,20]. The slow deactivation may occur by decomposition of the metal complexes within the hosting aluminosilicate involving oxidation exerted by the excess of hydrogen peroxide; according to Cardoso et al. [19], the deactivation of the catalytic centres can occur by decomposition of the complex inside the matrix by the oxidant. In this particular case, since the H_2O_2 is a very strong oxidizing agent, attack on the Mn–SALEN type complexes may take place by means of at least two ways: the disaggregation of the complex in the metal ion and the ligand predominantly by the change in the oxidation state of the metal centre, as well as the straightforward attack on the structure of the ligands, due to their organic nature. It could be also attributed to blocking of the active sites by products located in the pores of the catalysts or by side reactions leading to form μ-oxo-Mn(IV) dimeric units of the complexes, well known as inactive to catalyse cyclohexene epoxidation [54]. The used catalysts of method C ((IC)Al-PILC-U and (IIC)Al-PILC-IU) in corrected version) were characterized by FTIR spectroscopy after the first catalytic experiment (it is now shown as Fig. 1S, in Supplementary material) and compared against the corresponding catalysts before use ((IC)Al-PILC and (IIC)Al-PILC) and the starting isolated complexes (I) and (II). Such spectra basically showed that the signal of imine group weakens after the first catalytic cycle, though more drastically in the case of (IIC)Al-PILC-U than (IC)Al-PILC-U; in addition, a broadening of the signals was observed in the region 1565 cm^{-1} until around 1440 cm^{-1}, attributed to the stretch of aromatic linkage C=C, probably overlapped with a signal displayed in the same region by the vibration of deformation in water adsorbed on the starting clay (BVC) (see Fig. 3). It suggested that partial decomposition of both complexes took place after the first catalytic run, but with significant fraction of the immobilized complexes still active and stable within the catalyst's framework.

4. Conclusions

Two Mn(III) complexes with Schiff bases – [Mn(3,5-dtSALEN)Cl] and [Mn(3,5-dtSALHD)Cl] – were successfully synthesized with pretty high yields and featured the typical expected signals by UV–vis and FTIR and spectroscopies. Immobilization of both Mn complexes on a natural bentonite by three experimental approaches allowed to obtain six heterogeneized catalysts; simultaneous Al_{13}-pillaring/complex encapsulation of the aluminosilicate (method C) showed the highest Mn uptake efficiency exceeding 90%, against below 70% when every complex was directly adsorbed on the clay previously pillared by a conventional procedure (method A). The same immobilization procedure also led to enhanced basal spacing in the final materials and improved compensation of the cationic exchange capacity of the starting clay; indeed, it was observed that such a type of SALEN-like Mn(III) complexes incorporated by this procedure may significantly improve the intercalation of the starting clay by acting as pillar-spacers and leading to more homogeneous pillar distribution or by giving rise to highly aggregated, larger Al-based oligocations, able to expand the starting mineral to basal spacings beyond those typical of Al-pillared clays. The modified materials exhibited high catalytic performance in the bicarbonate-assisted cyclohexene epoxidation by hydrogen peroxide, in a cleaner reaction pathway with the catalytic species entrapped in a low cost inorganic hosting mineral and using a more environmental-friendly oxidizing agent than the usual iodosylbenzene. All materials reached conversions in the range 84–100% of the starting cyclohexene; the solids prepared by method C displayed the higher conversions of the olefin (up to 100%) and selectivities to the targeted epoxide (up to 77%), which decreased up to 85% when used in a second catalytic cycle, showing that pillars were able to keep trapped the active metal complexes in a great extent, though the typical structure of the metal complexes was partially affected by once finished the first catalytic cycle (according to FTIR of used materials).

Acknowledgements

Authors gratefully acknowledge funding by projects VIPRI—Nariño University (agreement 031/2009) and ID-3920 from Cauca University. V. Moreno thanks the grant received from COLCIENCIAS, program "Young Researchers". A. Gil and M.A. Vicente thank the support from the Spanish Ministry of Economy and Competitiveness (MINECO) and the European

Regional Development Fund (FEDER) (project MAT2013-47811-C2-R).

Appendix A. Supplementary data

Supplementary data associated with this article can be found, in the online version, at http://dx.doi.org/10.1016/j.molcata.2016.01.034.

References

[1] G. Franz, R.A. Sheldon, in: B. Elvers, S. Hawkins, G. Shulz (Eds.), Ullmann's Encyclopedia of Industrial Chemistry, vol. A, John Wiley and Sons, Inc., Weinheim, 1991, pp. 261–311.
[2] M.G. Clerici, G. Bellussi, U. Romano, J. Catal. 129 (1991) 159–167.
[3] S. Bhattacharjee, J.A. Anderson, J. Mol. Catal. A: Chem. 249 (2006) 103–110.
[4] U. Biermann, W. Friedt, S. Lang, W. Luhs, G. Machmuller, J.O. Metzger, M.R. Klaas, H.J. Schafer, M.P. Schneider, Angew. Chem. Int. Ed. 39 (2000) 2206–2224.
[5] M.A.R. Meier, J.O. Metzger, U.S. Schubert, Chem. Soc. Rev. 36 (2007) 1788–1802.
[6] A. Corma, H. García, Chem. Rev. 102 (2002) 3837–3892.
[7] K. Srinivasan, P. Michaud, J. Kochi, J. Am. Chem. Soc. 108 (1986) 2309–2320.
[8] R. Irie, K. Noda, Y. Ito, N. Matsumoto, T. Katsuki, Tetrahedron Lett. 31 (1990) 7345–7348.
[9] E. Jacobsen, W. Zhang, A. Muci, J. Am. Chem. Soc. 113 (1991) 7063–7064.
[10] T. Katsuki, Coord. Chem. Rev. 140 (1995) 189–214.
[11] I. García-Bosch, X. Ribas, M. Costas, Adv. Synth. Catal. 351 (2009) 348–352.
[12] D.E. De Vos, M. Dams, B.F. Sels, P.A. Jacobs, Chem. Rev. 102 (2002) 3615–3640.
[13] P. Das, I. Kuźniarska-Biernacka, A.R. Silva, A. Carvalho, J. Pires, C. Freire, J. Mol. Catal. A: Chem. 248 (2006) 135–143.
[14] D. Chatterjee, A. Mitra, J. Mol. Catal. A: Chem. 144 (1999) 363–367.
[15] B. Choudary, N. Sreenivasa, M. Lakshmi, P. Lakshmi, Catal. Lett. 76 (2001) 213–218.
[16] I. Kuźniarska-Biernacka, A. Silva, A. Carvalho, J. Pires, C. Freire, Langmuir 21 (2005) 10825–10834.
[17] B. Cardoso, A.R. Silva, B. Castro, C. Freire, Appl. Catal. A 285 (2005) 110–118.
[18] K. Yu, Z. Gu, R. Ji, L.-L. Lou, S. Liu, Tetrahedron 65 (2009) 305–311.
[19] B. Cardoso, J. Pires, A. Carvalho, I. Kuzniarska-Biernacka, A. Silva, B. Castro, C. Freire, Microporous Mesoporous Mater. 86 (2005) 295–302.
[20] B. Cardoso, J. Pires, A.P. Carvalho, I. Kuźniarska-Biernacka, A.R. Silva, C. Freire, B. de Castro, Eur. J. Inorg. Chem. 5 (2005) 837–844.
[21] L. Gandía, M.A. Vicente, A. Gil, Appl. Catal. A 196 (2000) 281–292.
[22] M.A. Vicente, R. Trujillano, K.J. Ciuffi, E.J. Nassar, S.A. Korili, A. Gil, et al., Pillared Clays and Related Catalysts, in: A. Gil (Ed.), Springer, Berlin, 2010, pp. 301–318.
[23] T. Luts, W. Suprun, D. Hofmann, O. Klepel, H. Papp, J. Mol. Catal. A: Chem. 261 (2007) 16–23.
[24] G. Nagendrappa, Appl. Clay Sci. 53 (2011) 106–138.
[25] L.A. Galeano, M.A. Vicente, A. Gil, Catal. Rev. 56 (2014) 239–287.
[26] A. Gil, S.A. Korili, R. Trujillano, M.A. Vicente, Appl. Clay Sci. 53 (2010) 97–105.
[27] S. Arellano, T. Gallardo, T. Osorio, Rev. Soc. Quim. Mex. 44 (2000) 204–208.
[28] G. Johansson, Acta Chem. Scand. 14 (1960) 771–773.
[29] F. Figueras, Catal. Rev. 30 (1988) 457–499.
[30] R. Mokaya, W. Jones, J. Catal. 172 (1997) 211–221.
[31] I. Kuźniarska-Biernacka, A.R. Silva, R. Ferreira, A.P. Carvalho, J. Pires, C. Freire, B. de Castro, New J. Chem. 28 (2004) 853–858.
[32] G. Grigoropoulou, J.H. Clark, J.A. Elings, Green Chem. 5 (2003) 1–7.
[33] R.A. Sheldon, Top. Curr. Chem. 164 (1993) 21–34.
[34] B.S. Lane, M. Vogt, V.J. De Rose, K. Burgess, J. Am. Chem. Soc. 124 (2002) 11946–11954.
[35] M. Ghorbanloo, H.H. Monfared, C. Janiak, J. Mol. Catal. A: Chem. 345 (2011) 12–20.
[36] B. Qi, X.-H. Lu, D. Zhou, Q.-H. Xia, Z.-R. Tang, S.-Y. Fang, T. Pang, Y.-L. Dong, J. Mol. Catal. A: Chem. 322 (2010) 73–79.
[37] L.A. Galeano, A. Gil, M.A. Vicente, Appl. Catal. B 100 (2010) 271–281.
[38] A. Silva, C. Freire, B. De Castro, New J. Chem. 28 (2004) 253–260.
[39] A. Silva, V. Budarin, J. Clark, B. De Castro, C. Freire, Carbon 43 (2005) 2096–2105.
[40] J. Cubillos, S. Vásquez, C. Montes De Correa, Appl. Catal. A 373 (2010) 57–65.
[41] A. Chellamani, P. Kulanthaipandi, S. Rajagopal, J. Org. Chem. 64 (1999) 2232–2239.
[42] L.A. Galeano, A. Gil, M.A. Vicente, App. Catal. B 104 (2011) 252–260.
[43] R. Ji, K. Yu, L.-L. Lou, Z. Gu, S. Liu, J. Inorg. Organomet. Polym. Mater. 20 (2010) 675–683.
[44] S. Bi, C. Wang, Q. Cao, C. Zhang, Coord. Chem. Rev. 248 (2004) 441–455.
[45] H. Yao, D.E. Richardson, J. Am. Chem. Soc. 122 (2000) 3220–3221.
[46] G. Salomao, M. Olsen, V. Drago, C. Fernandes, L. Cardozo, O. Antunes, Catal. Commun. 8 (2007) 9–72.
[47] J. Huang, J. Cai, C.M. Li, X. Fu, Inorg. Chem. Commun. 44 (2014) 20–24.
[48] M.B. Ansari, E.-Y. Jeong, S.-E. Park, Green Sustain. Chem. 2 (2012) 1–7.
[49] A. Costa, G. Ghesti, J. de Macedo, V. Braga, M. Santos, J. Dias, S. Dias, J. Mol. Catal. A: Chem. 282 (2008) 149–157.
[50] S. Alavi, H. Hosseini-Monfared, M. Siczek, J. Mol. Catal. A: Chem. 377 (2013) 16–18.
[51] J.M. Fraile, J.I. García, J. Massam, J.A. Mayoral, J. Mol. Catal. A: Chem. 136 (1998) 47–57.
[52] G. Oxford, D. Dubbeldam, L. Broadbelt, R. Snurr, J. Mol. Catal. A: Chem. 334 (2011) 89–97.
[53] R. Sheldon, J. Van Doorn, J. Catal. 31 (1973) 427–437.
[54] D.D. Agarwal, R.P. Bhatnagar, R. Jain, S. Srivastava, J. Chem. Soc. Perkin Trans. 2 (1990) 989–992.